Hindawi
Journal of Sensors
Volume 2017, Article ID 4198485, 6 pages
https://doi.org/10.1155/2017/4198485

Research Article

Fabricating 90 nm Resolution Structures in Sol-Gel Silica Optical Waveguides for Biosensor Applications

Yasufumi Enami

School of System Engineering, Kochi University of Technology, 185 Miyanoguchi, Tosayamada, Kami, Kochi 782-8502, Japan

Correspondence should be addressed to Yasufumi Enami; enami.yasufumi@kochi-tech.ac.jp

Received 10 February 2017; Accepted 14 March 2017; Published 23 April 2017

Academic Editor: Zubair Ahmad

Bragg grating structure in a sol-gel silica waveguide is fabricated on the basis of nanoimprint lithography for biophotonic applications. The process realizes nonstandardized lithography in sol-gel silica at a high resolution for a relatively large area in the range of several micrometers with a resolution in the order of several nanometers. Here we demonstrate structures of 250 and 90 nm resolutions in a sol-gel silica optical waveguide for a large area that is not optimized to date. Bragg grating of a 250 nm periodic structure is realized for a 1 mm long area.

1. Introduction

Sol gel silica materials have been extensively used in photonic waveguide devices such as electrooptic (EO) modulators [1, 2], biophotonic sensors [3], and other sensors [4, 5]. Green fluorescent protein- (GFP-) doped sol-gel silica waveguide was used in biophotonic sensors to detect organophosphorus (OP) compound when the blue laser pumps the waveguide to extract green light from the waveguide [3]. Bragg grating in an optical waveguide reflects (or transmits) the waveguiding light at a specific wavelength, which works as a reflector at a narrow wavelength in optical devices such as laser diode. Fluorescent light in the waveguide can be returned, amplified, and oscillated at a specific wavelength between two Bragg gratings [6]. The sensitivity of the biophotonic sensors increases when Bragg grating structure is fabricated in the sol-gel waveguide core. Multiple waveguides can be serially coupled to single-mode fibers and can be used as sensing parts to remotely and distributively detect OP compound. Therefore, fabrication of Bragg grating in the sol-gel waveguides with the same resolution and shorter time is preferred compared with standard electron beam lithography. Optimizing these devices requires fabricating high-resolution sol-gel silica structures. Motivated by this demand, I herein report a technique to fabricate periodic sol-gel silica structures containing 250 nm and 90 nm structures, which represents the structure with the highest resolution yet fabricated in a sol-gel silica waveguide and would be suitable for biophotonic sensors.

Sol-gel silica planar single-mode (SM) waveguides incur a much lower coupling loss (e.g., 0.1 dB) than other optical waveguides that comprise semiconductor materials and polymers when coupled with SM fibers, and waveguide propagating loss is also much lower (e.g., 1 to 2 dB/cm^2). Sol-gel silica waveguides accept living cells of any size, for example, green fluorescent protein [3], which emits green light when exposed to blue light coupled into the waveguide. Hybrid EO polymer/sol-gel silica waveguide modulators have a two-component waveguide core, wherein the EO polymer core is deposited on the sol-gel silica core [1, 2]. The EO polymer was laterally confined between the side walls of the top sol-gel silica cladding that was fabricated as a window for the selectively buried sol-gel silica core. In modulator devices, the EO polymer must be electrically poled by using a high poling voltage with the polymer at its glass-transition temperature. In EO polymer waveguide modulators, as some sol-gel silica thin films have a conductivity over an order of magnitude greater than that of the EO polymer in hybrid EO polymer/sol-gel silica waveguide modulators, the higher poling voltage creates the maximum possible poling electric field in the EO polymer, which leads to the lowest half-wave voltage of 0.65 V for EO modulators [1].

Sol-gel silica waveguides have been used as biophotonic sensors to detect organophosphorus compounds such as sarin and insecticide. Such detection is possible because of live green fluorescent protein and organophosphorus hydrolase on a yeast cell at distances of few nanometers, which is directly doped into the sol-gel silica core [3]. Organophosphorus hydrolase chemically reacts with organophosphorus compound, which changes pH near the green fluorescent protein and organophosphorus hydrolase. When blue light is coupled into the green-fluorescent-protein-doped sol-gel silica waveguide, the proteins fluoresce green light and light is coupled out of the waveguide. The lifetime of the device is one month, and the intensity of the green light changes when pH near GFP is changed. When organophosphorus compound approaches organophosphorus hydrolase doped in the waveguide sensor, it changes its pH near GFP, which results in a change in the output intensity of green fluorescent light. Therefore, when the end facets of multiple waveguides are connected to optical fibers that transmit the blue input light and green output light, the sol-gel waveguides may be used to remotely detect the organophosphorus compound.

Photopatterning the sol-gel silica material itself does not require other materials, such as a photoresist. Although sol-gel silica waveguides have many advantages, the resolution of a sol-gel silica photopatterned structure is more than a few μm when standard photolithographic methods are applied. Previous nanoimprint methods for sol-gel silica have been hard pressed to create structures less than 500 nm wide [7–10]. In this work, I obtained resolutions of 90 and 250 nm for sol-gel silica materials for photonic applications such as ring resonators and Bragg grating waveguides. The nanoimprint method is preferred for photopatterning photonic waveguide devices; this method is based on Si stamps fabricated with a resolution exceeding 100 nm because of electron beam (EB) lithography. Electron beam lithography is typically used for Si dry etching, and it is not optimized for other materials such as sol-gel silica and other glasses. Moreover, more time is required to apply it to non-Si materials such as sol-gel silica. Thus, using EB lithographic patterning with an EB resist to write an EB pattern with high resolution takes a relatively long time. The nanoimprint method, on the other hand, reduces the time and also the cost. In addition, the sol-gel silica cannot crack as the Si stamp is fabricated independently with the EB method, and the stamp can be used to produce multiple devices from non-Si materials.

A sol-gel silica thin film is spin-coated onto a thermally oxidized and hydrolyzed Si substrate and a silica (SiO_2) network forms when the film is irradiated with ultraviolet (UV) light [2]. The thin film of the sol-gel silica begins to form SiO_2 because hydrolysis of the sol-gel silica is initiated by UV radiation or heating of the film. The liquid state (sol) of the sol-gel silica changes to solid state (gel) due to hydrolysis. Therefore, when UV light irradiates the sol-gel thin film through a photomask and the sol-gel film is dissolved in an organic solvent, the UV-irradiated parts remain intact on the substrate and form a patterned optical waveguide with the resolution of 1 to 2 μm. The index of refraction of sol-gel silica is near 1.50 and the width of the sol-gel waveguide core is in the range of 4 to 8 μm, which satisfies the single-mode

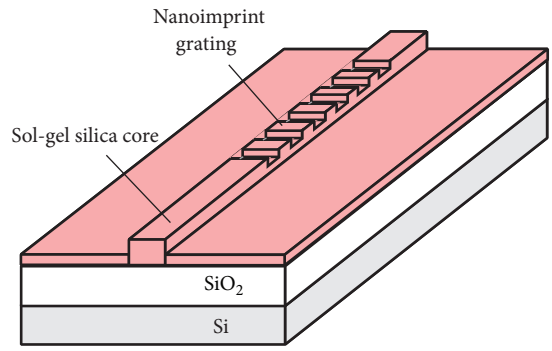

Figure 1: Schematic of grating structure fabricated in sol-gel silica waveguide by using the nanoimprint method. The sol-gel silica core was deposited on the SiO_2-Si substrate, following which the grating structure was nanoimprinted on the sol-gel silica core.

condition at a wavelength of 1.55 μm. When the index of refraction of the sol-gel silica is modified by doping (e.g., zirconium peroxide), the difference in the index of refraction between the sol-gel silica core and the thermally oxidized SiO_2 substrate may be finely controlled to minimize coupling losses with other devices, such as standard single-mode fibers [1–3].

When two Bragg gratings are fabricated on a sol-gel silica waveguide [11–13], blue light is confined in the waveguide and fluorescence at 520–540 nm originating in the waveguide begins lasing between the gratings in a narrow wavelength range; the structure forms a distributed feedback laser. The sensitivity to detect biomaterials increases when the grating structure is fabricated, although the single Bragg grating structure is already fabricated. This configuration therefore improves the detection sensitivity for both single-grating and double-grating resonators. For the present work, we fabricated a Mach-Zehnder (MZ) type sol-gel silica waveguide to detect a virus when an antibody is attached to a branch of MZ sol-gel silica waveguide. The antibody that captured the virus changes the refractive index of the sol-gel silica core in the waveguide. The MZ waveguide has one input and one output, which separates the input waveguiding light to two branches in the middle of the waveguide and combines the separated light at the end of the waveguide. Therefore, when the refractive index of one waveguide branch is changed, the transmitted light through the branch suffers phase delay in the waveguide. Conversely, the waveguiding light in another branch does not suffer phase delay because the refractive index of the branch is not changed. Finally, the waveguiding light combined before the output and changes the optical intensity. In this case, we used the wavelength of 1.55 μm to construct a long-haul-fiber virus-sensing network wherein a Bragg grating and ring resonator increase the detection sensitivity instead of our recently employed MZ waveguide. I designed the Bragg grating in the sol-gel silica waveguide for the wavelength of 1.55 μm (see Figure 1) and estimated grating width of 258 nm and grating spacing of 259 nm (one period is 517 nm) for use with the telecom wavelength range of 1450–1590 nm. The effective index of refraction of the sol-gel silica waveguide was estimated to be 1.49 for the

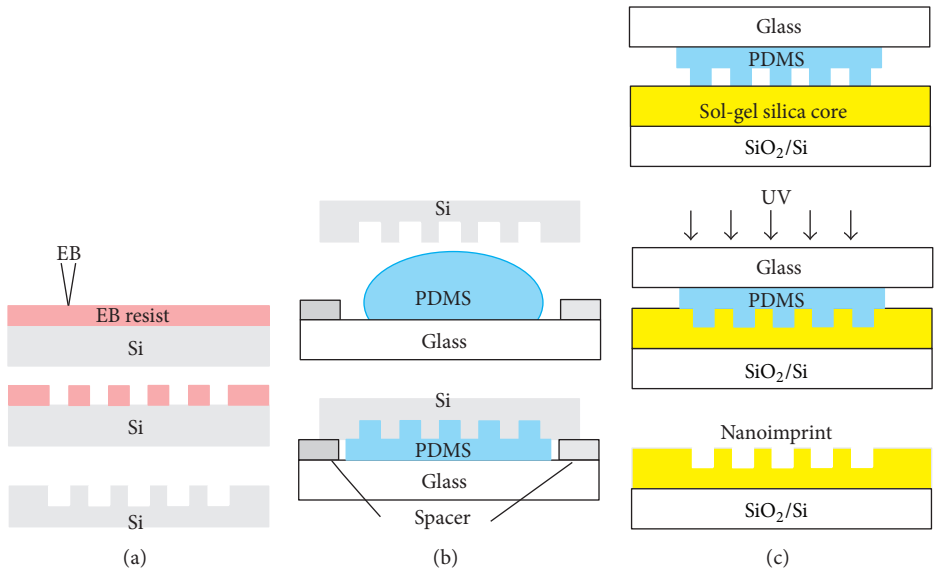

FIGURE 2: Schematic of nanoimprint process on sol-gel silica core. (a) Si master stamp was dry-etched for patterning after electron beam (EB) resist was EB-radiated and developed in a developer. (b) Si master stamp was pressed on polydimethylsilane (PDMS) and baked while maintaining equal spacing with the spacers. After baking, the PDMS stamp was duplicated. (c) The PMDS stamp was attached and pressed on the sol-gel silica core. The sol-gel silica core was nanopatterned when the PDMS stamp was pressed on the core and irradiated with UV light. Finally, the PDMS stamp was removed and baked.

transverse electric (TE) mode. I also fabricated a periodic 90 nm structure (width of 90 nm and period of 93 nm), which represents the structure with highest resolution yet achieved with sol-gel silica for a Bragg grating at the wavelength of 550 nm.

The Bragg grating was fabricated by using the nanoimprinting process (see Figure 2). The first step was to fabricate, with high resolution, the Si wafer master stamp, which was used in all following process, as shown in Figure 2(a). After the Si wafer was cleaned by using a mixed acid (H_2SO_4 and H_2O_2 at a 3 : 1 volume ratio), a 320 nm thick positive EB resist (Zeon ZEP520A) was spin-coated on the Si wafer at a rotation speed of 5 krpm. The EB resist was baked at 200°C for 5 min and is then exposed to a 10 nm wide EB line by using an EB lithography system (Elionix ELS-7500EX). After the EB exposure, the EB resist was developed by using the developer Zeon ZED-N50. The EB resist was then baked at 140°C for 3 min for consecutive O_2 ashing. The Si wafer with the nanopatterned EO resist was then dry-etched in a mixed-gas flow of SF_6 at 90 sccm (standard cubic centimeters per Minute), C_4F_8 at 10 sccm, and O_2 at 5 sccm by using reactive-ion etching (SAMCO RIE-800iPB). The etching depth in the Si wafer was estimated to be 110 to 130 nm from the etching rate of 1.125 nm/s and an etching time of 98 to 116 s. After etching Si, the EB resist was removed by using an ashing machine (SAMCO RIE-10NR).

Polydimethylsilane (PDMS), which was widely used for nanoimprinting, was dropped onto a microscope glass slide with 5 mm thick Si spacers, as shown in Figure 2(b). The Si master stamp was pressed onto the PDMS with a 0.5 mm space imposed by a spacer fixed between the Si stamp and the glass; this was the most important process to obtain a proper nanoimprint with large field size (~10 mm × 5 mm) in the subsequent nanoimprint step for the sol-gel waveguide. In an initial trial, I found it difficult to nanoimprint over a large area without using spacers, even though small areas of the imprint contained fine structure. After pressing the Si stamp onto the PDMS to transfer the nanoscale structure, the PDMS was baked at 80°C for 2 h with the Si stamp held in place.

A 0.9 μm thick core film is spin-coated onto a 6 μm thick silica-on-silicon substrate and soft baked at 90°C for 10 min. Radiation from the mercury *i* line (365 nm, 10 mW/cm^2) was delivered from a mask aligner (Karl Suss MJB3) to the sol-gel layer through a photomask to etch a 4 μm wide core region. The regions exposed to UV irradiation became cross-linked to form a silica network and are insoluble in isopropanol, which was used as a wet etchant. An additional core layer of 0.9 μm thick sol-gel silica was spin-coated onto the sol-gel core at the speed of 2000 rpm for 30 s to fabricate the grating structure, which was soft baked at 90°C for 10 min for nanoimprinting by using the PDMS stamp. The PDMS stamp on the glass substrate was attached to the sol-gel core, which was UV-irradiated in the mask aligner for 5 min. After the PDMS stamp was removed, the nanoimprinted sol-gel silica waveguide was hard baked at 150°C for 1 h.

A 250 nm wide sol-gel silica structure and a 90 nm wide sol-gel silica structure were fabricated by using nanoimprinting and were imaged by using a scanning electron microscopy (SEM; see Figure 3). The cross section of the structures was approximately 100 nm high for 250 nm. The 250 nm wide structure was imaged over a large field of ~10 mm × 5 mm and showed uniform fine structure (see Figure 3(a)). The expanded SEM image in Figure 3(b) shows a part of the 252 nm wide, ~60 nm high structure, which has a periodicity

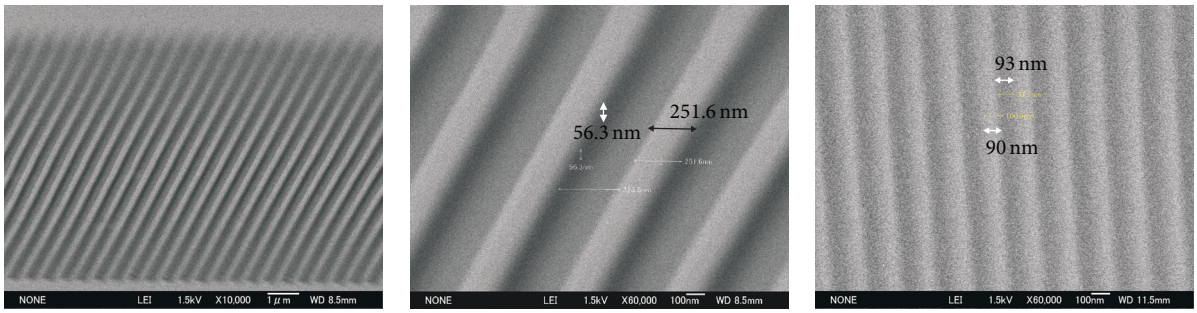

(a) (b) (c)

FIGURE 3: SEM image of nanoimprinted sol-gel silica core. (a) Large area image of periodic structure. (b) Expanded view of periodic structure showing the grating with approximately 250 nm wide periodic structure and approximately 250 nm periodicity. (c) Approximately 90 nm wide periodic structure.

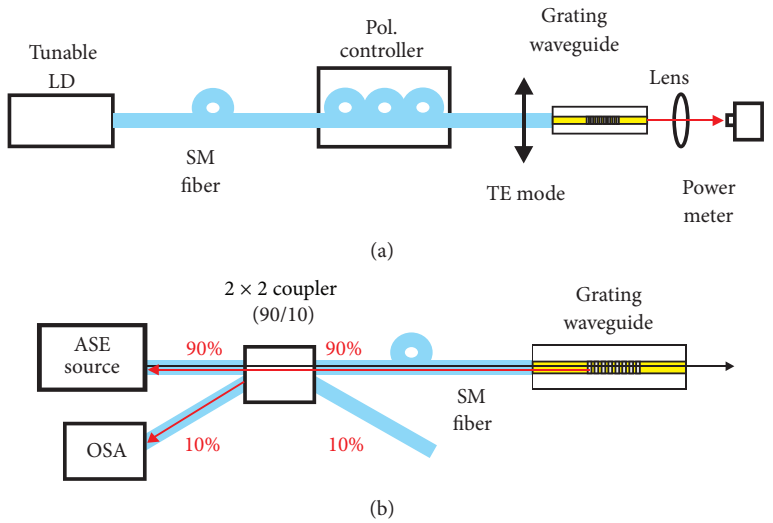

FIGURE 4: Experimental setup for measuring optical spectrum. (a) Measurement of optical transmission spectrum coupling tunable TE laser into the waveguide grating and the measuring light transmitted through the waveguide with power meter. (b) Measurement of optical reflection spectrum by coupling amplified spontaneous emission into waveguide grating through the 2 × 2 coupler and detecting reflected light with optical spectrum analyzer (OSA).

of ~550 nm. I also imaged a 90 nm wide, ~60 nm high structure with higher resolution, which will be used as a Bragg grating for shorter wavelengths (e.g., 550 nm). To the best of our knowledge, the 90 nm wide, 60 nm high periodic structure is one of the highest resolution sol-gel silica thin film structures ever fabricated.

I thus fabricated a SM sol-gel silica waveguide with a Bragg grating on the SiO_2/Si substrate with a design wavelength band of 1450–1590 nm. The waveguide comprises a 4 μm wide, 1.8 μm high sol-gel silica core with a ~250 nm width, a ~60 nm deep, 1 mm long grating structure (see Figure 1). The waveguide was cleaved to form a 5 mm long waveguide with an Si substrate. I measured the transmission spectrum through the sol-gel waveguide by using a tunable laser diode with a wavelength of 1510–1610 nm, as shown in Figure 4(a). The input light was controlled and the TE polarized by using a polarization controller; the output light of the waveguide was collected by 20x microscope objective lens and focused onto a power meter. The reflected spectrum was measured separately by using the amplified spontaneous emission (ASE) and an optical spectrum analyzer, as shown in Figure 4(b). The ASE output was randomly polarized and so could not be used to measure the transmission spectrum because the Bragg grating was designed to reflect only TE-polarized light and transit transverse-magnetic (TM) polarized light. Because the optical power of the randomly polarized light transmitted through the waveguide grating exceeded that of the transmitted TE light, the optical spectrum between the TE mode and other polarized modes could not be distinguished. The transmission and reflection spectra thus obtained are shown in Figure 5. The reflected light that was measured by using the optical setup shown in Figure 4(b) was normalized to obtain the reflection spectrum after accounting for the optical loss induced by a 2 × 2 coupler,

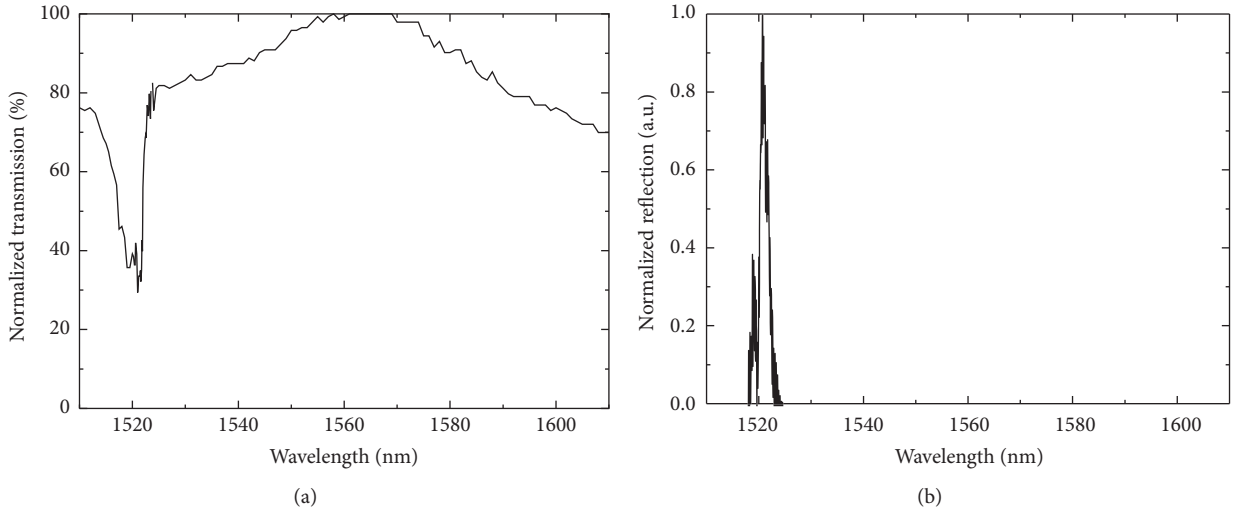

Figure 5: Normalized optical power. (a) Transmission spectrum of the Bragg grating in the sol-gel silica waveguide. (b) Reflection spectrum of the grating.

by the coupling between the fibers and waveguide, and by waveguiding propagation. The shortest wavelength transmitted was 1521.6 nm, which was matched to the wavelength of 1521.672 nm for the highest-wavelength reflection, as shown in Figure 5. The whole grating strucuture was designed to consist of 1063 gratings, which has the width of 258 nm and the spacing of 259 nm, which corresponds to a relatively low reflectivity. However, when the spacing number exceeds 10,000, I calculate that the reflection should be maximized.

In summary, I successfully fabricated 258 and 90 nm periodic structures in a sol-gel silica waveguide core. The effectiveness of the grating structure in the waveguide was examined based on transmission and reflection spectra for laser light at 1.55 μm coupled into the waveguide. The transmission and reflection spectra show that the imprint process was successful in fabricating the waveguide grating. The fabricated periodic structure for the 250 and 90 nm lines represents the structure with the highest resolution yet fabricated in a sol-gel silica waveguide and would be suitable for biophotonic sensors. I did not examine the limitation of the resolution of the nanoimprint lithography for the sol-gel silica waveguide in this work. Higher resolution would be examined when the structure in the Si master stamp is fabricated using a more sophisticated method. The nanoimprint method in the sol-gel silica waveguide would be applied for biosensor and photonic applications.

2. Experimental Section

Regarding sol-gel silica solution, for the waveguide core, a sol-gel solution was prepared which consisted of methacryloyloxy propyltrimethoxysilane (MAPTMS) and an index modifier (zirconium(IV)-*n*-propoxide) at a molar ratio of 85 (MAPTMS)/15 mol%. A 0.1 N HCl solution was used as catalyst, and Irgacure 184 (Ciba) was used as a photoinitiator for the side-cladding solutions to accelerate hydrolysis of the silica for subsequent wet etching in isopropanol.

Conflicts of Interest

The author declares that there are no conflicts of interest regarding the publication of this paper.

Acknowledgments

This work was supported by a Grant-in-Aid for Scientific Research (A) (Grant no. 21246060 and no. 24246063) from MEXT, Japan, and JST A-STEP. The author is grateful to Mr. H. Nakamura and Dr. Y. Jouane in University of Strasbourg, France, for their support in conducting the experiments.

References

[1] Y. Enami, D. Mathine, C. T. DeRose et al., "Hybrid cross-linkable polymer/sol-gel waveguide modulators with 0.65 V half wave voltage at 1550 nm," *Applied Physics Letters*, vol. 91, no. 9, Article ID 093505, 2007.

[2] Y. Enami, C. T. DeRose, D. Mathine et al., "Hybrid polymer/sol-gel waveguide modulators with exceptionally large electro-optic coefficients," *Nature Photonics*, vol. 1, pp. 180–185, 2007.

[3] Y. Enami, K. Tsuchiya, and S. Suye, "Detection of organophosphorus compound based on a sol-gel silica planar waveguide doped with a green fluorescent protein and an organophosphorus hydrolase," *Applied Physics Letters*, vol. 98, no. 23, Article ID 233503, 2011.

[4] B. Bhola, P. Nosovitskiy, H. Mahalingam, and W. H. Steier, "Sol-gel-based integrated optical microring resonator humidity sensor," *IEEE Sensors Journal*, vol. 9, no. 7, pp. 740–747, 2009.

[5] F. Pang, X. Han, F. Chu et al., "Sensitivity to alcohols of a planar waveguide ring resonator fabricated by a sol-gel method," *Sensors and Actuators B: Chemical*, vol. 120, no. 2, pp. 610–614, 2007.

[6] Y. Enami, "Sol-gel silica waveguide for biophotonic sensors," Technical Digest W4A5, Optical Society of America, 2016.

[7] C. Becker, P. Wyss, D. Eisenhauer et al., "5×5 cm^2 silicon photonic crystal slabs on glass and plastic foil exhibiting

broadband absorption and high-intensity near-fields," *Scientific Reports*, vol. 4, article 5886, 2014.

[8] G. Brusatin and G. Della Giustina, "Hybrid organic-inorganic sol-gel materials for micro and nanofabrication," *Journal of Sol-Gel Science and Technology*, vol. 60, no. 3, pp. 299–314, 2011.

[9] C. Peroz, V. Chauveau, E. Barthel, and E. Søndergård, "Nanoimprint lithography on silica sol-gels: a simple route to sequential patterning," *Advanced Materials*, vol. 21, no. 5, pp. 555–558, 2009.

[10] A. Moujoud, H. J. Kim, S. H. Kang et al., "Double component long period waveguide grating filter in sol-gel material," *Optics Express*, vol. 15, no. 23, pp. 15147–15153, 2007.

[11] M. Thiel, G. Flachenecker, and W. Schade, "Femtosecond laser writing of Bragg grating waveguide bundles in bulk glass," *Optics Letters*, vol. 40, no. 7, pp. 1266–1269, 2015.

[12] M. A. Fardad, H. Luo, Y. Beregovski, and M. Fallahi, "Solgel grating waveguides for distributed Bragg reflector lasers," *Optics Letters*, vol. 24, no. 7, pp. 460–462, 1999.

[13] P. Prosposito, C. Palazzesi, F. Michelotti, V. Foglietti, and M. Casalboni, "Hybrid solgel Bragg grating loaded waveguide by soft-lithography and its potential use as optical sensor," *Journal of Sol-Gel Science and Technology*, vol. 60, no. 3, pp. 395–399, 2011.